Supporting Information

# Crystallization-Driven Self-Assembly of Poly(3-hexylthiophene)-*b*-Poly(2,5-bis(2-ethylhexyloxy)p-phenylene), a π-Conjugated Diblock Copolymer with a Rigid Rod Corona-Forming Block

**Authors:** Marcus Vespa[1], Liam MacFarlane[1], Zachary M. Hudson[2*], and Ian Manners[1,†]

**Affiliations:** [1]Department of Chemistry, University of Victoria, 3800 Finnerty Rd, Victoria, British Columbia V8W 3V6, Canada

[2]Department of Chemistry, The University of British Columbia, Vancouver, British Columbia V6T 1Z1, Canada

*Correspondence to: zhudson@chem.ubc.ca

**Contents**

## Materials and Methods

All reagents used for polymer synthesis were of reagent grade and were used as received unless otherwise stated. All the air-free chemistry was performed in a dinitrogen-filled ($N_2$) MBraun 200B glovebox equipped with a cold-well or on a dinitrogen Schlenk line using standard techniques. 2-Ethyhexyl bromide, isopropylmagnesium chloride – lithium chloride (*i*PrMgCl•LiCl) (1.3M in THF), potassium carbonate, and 2,5-dibromohydroquinone (97%) were purchased from Millipore Sigma. 2,5-dibromo-3-hexylthiophene was purchased from Combiblocks and distilled under reduced pressure before use. Solvents were dried and de-oxygenated using a Solvent Purification System (SPS).[1] Ni(*o*-tolyl)(dppe)Cl was synthesized as previously reported.[2] Self-assembly experiments were performed using HPLC grade solvents and the solvents were filtered through a 0.2 µm polytetrafluoroethylene membrane.

### Nuclear magnetic resonance (NMR)

$^1$H NMR spectra were taken with a Bruker 500 MHz spectrometer; chemical shifts were referenced to the residual proteosolvent peak ($CHCl_3$, $\delta$ = 7.26 ppm).

### Gel Permeation Chromatography (GPC)

GPC was conducted using a Malvern Omnisec Resolve/Reveal equipped with an automatic sampler, pump, injector, inline degasser column oven (set at 35 °C), elution columns consisting of styrene/divinylbenzene gels (of pore size 500–5,000 Å), refractometer, four capillary differential viscometer, UV/Vis detector ($\lambda$ = 440 nm) and dual angle laser light scattering detector (7° and 90°). GPC grade THF with 1 wt% triethylamine was used as the eluent, with a set flow rate of 1 mL/min. BCP samples were dissolved in THF at 1 mg/mL and filtered through a 0.2 µm poly(tetrafluoroethylene) membrane prior to analysis. Homopolymer concentration was

2 mg/mL in THF and sample was filtered through a 0.2 μm poly(tetrafluoroethylene) membrane prior to analysis.

**Preparatory GPC**

Preparatory gel permeation chromatography was performed on a Shimadzu Prep GPC equipped with a CBM-20A communications bus module, LC-20AP solvent delivery unit, SIL-10AP autosampler, CTO-40C column oven, SPD-40 UV/Vis detector, RID-20A refractive index detector, and FRC-10A fraction collector. An initial injection of polymer in THF (1 mL, 10 mg/mL) at a flow rate of 3 mL/min using HPLC grade THF as eluent was used to gather the retention times of the species in solution. Using this data, the fraction collector was calibrated to separate the desired peaks into separate vials. Subsequent injections (3 mL, 10 mg/mL, 3 mL/min) were repeated until the desired volume was collected. The resulting solutions were concentrated *in vacuo* to yield the final polymers. Removal of homopolymers was assessed using UV-detection on the Malvern Omnisec GPC and thin layer chromatography.

**Transmission Electron Microscopy (TEM)**

Carbon films were deposited onto freshly cleaved mica sheets using a Leica EM ACE600 sputter/carbon coater instrument. Carbon films were deposited onto copper grids (500 mesh) purchased from Ted Pella, Inc. by floatation on water and allowed to dry over 24 h. Samples for electron microscopy were prepared by drop-casting 10 μL of self-assembly solution onto a TEM grid placed on filter paper to absorb the excess solution. Bright field TEM images were obtained using a JEOL JEM 1011 operating at 80 kV, equipped with a Gatan Orius SC1000 CCD camera. Nanofiber lengths and widths were analysed using ImageJ, an open source software package developed at the US National Institute of Health.[3] Approximately 150 micelles were traced by hand to determine contour lengths that were then used to calculate the number-averaged length

($L_n$) and weight-average length ($L_w$) according to equations 1 and 2 where $L$ = object length and $N$ = number. Fiber length distribution was calculated by $L_w/L_n = Đ_L$.

The number-average length ($L_n$) and weight-average length ($L_w$) were calculated according to the following equations:

$$(1)\ L_n = \frac{\sum_i^n N_i L_i}{\sum_i^n N_i} \qquad (2)\ \ L_w = \frac{\sum_i^n N_i L_i^2}{\sum_i^n N_i L_i}$$

Number-averaged width ($W_n$) was calculated according to equation 3 where $W$ = object width and $N$ = number.

$$(3)\ W_n = \frac{\sum_i^n N_i W_i}{\sum_i^n N_i}$$

**Sonication**

Sonication bath: Nanofiber sonication was carried out using a Fisherbrand FB11203 sonication bath (37 kHz sonication frequency and 100% power) with the sweep function on and the bath temperature at 0 °C.

Sonotrode: Nanofiber sonication was carried out using a Heischler UP100H ultrasonic processor affixed with a titanium sonotrode probe at 100% power.

**Variable-temperature UV/Vis absorption spectroscopy (VT-UV/Vis)**

VT-UV/vis data was obtained on a Cary 100 spectrometer equipped with a Peltier temperature controller employing quartz cells (1 cm x 0.1 cm) from 200 to 800 nm. Experiments were conducted at a concentration of 0.05 mg/mL to allow for convenient monitoring of fiber-like micelle formation and dissolution.

**Wide-Angle X-ray Spectroscopy (WAXS)**

Reciprocal space maps were collected with a Pixcel 3D detector on an Empyrean diffractometer (Panalytical) equipped with a Cu Kα1 (λ = 1.5406 Å) source powered at 45 kV and 40 mA.

**Atomic Force Microscopy (AFM)**

AFM analysis was obtained using a 5500 Atomic Force Microscope (Agilent Technologies). The images were recorded in AC mode with a scanning speed of 1.0 μm/s in an area of 4.0 $\mu m^2$ at 1024 × 1024 resolution. The tips employed (Tap150Al-G, Budget Sensors) consisted of a conical silicon tip with aluminum reflective coating and a resonance frequency and spring force constant of 150 kHz and 5 N/m, respectively. The samples for AFM were prepared on a silicon wafer by drop-casting the nanofiber solution (in 100 % *n*BuAc, 20 μL, 0.05 mg/mL) onto the clean silicon wafer. The silicon wafer was gently dried from the sides with a filter paper and dried via vacuum desiccation.

## Experimental Procedures

**Scheme S1. Synthesis of 1,4-dibromo-2,5-bis(2-ethylhexyloxy)benzene**

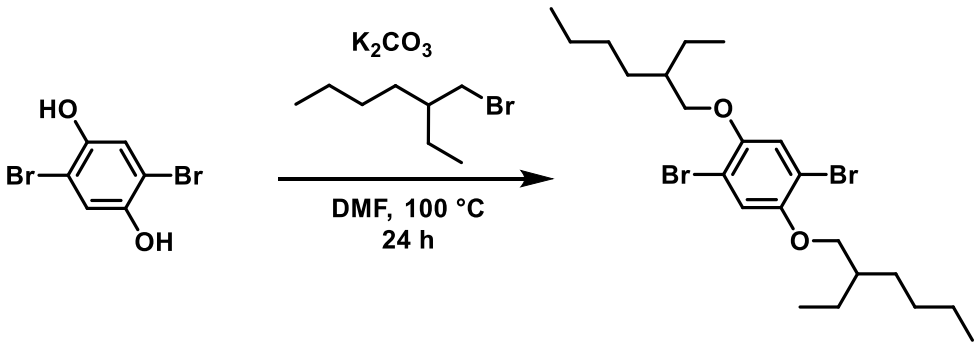


This product was synthesized using a previously published procedure from reference.[4] (6.73 g, 91% yield).

**Scheme S2. Synthesis of P3HT$_{35}$-*b*-PPP$_{15}$**

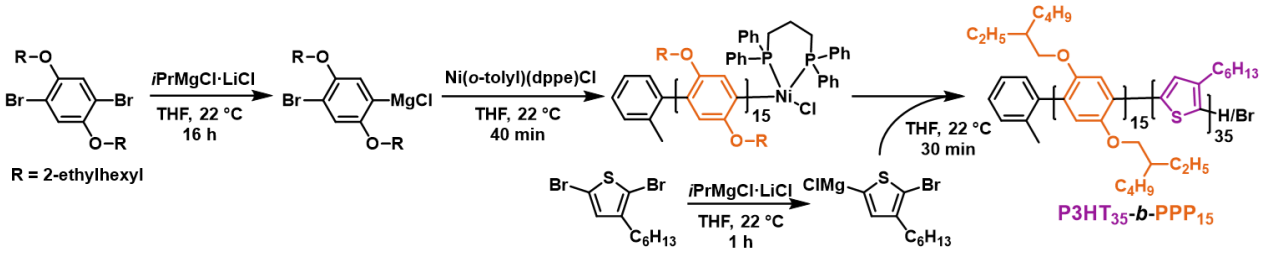


In a $N_2$-filled glovebox, a dry 100-mL Schlenk flask affixed with a stir bar was charged with 1,4-dibromo-2,5-bis(2-ethylhexyloxy)benzene (1.02 g, 2.05 mmol, 45 equiv.) and dry tetrahydrofuran (THF) (10 mL) was added. iPrMgCl·LiCl (1.3 M in THF, 1.62 mL, 2.11 mmol, 46 equiv.) was added dropwise and the solution was stirred for 16 h resulting in a faint yellow solution. In a separate dry 100-mL Schlenk flask affixed with a stir bar, 2,5-dibromo-3-hexylthiophene (0.448g, 1.37 mmol, 30 equiv.) was dissolved in dry THF (10 mL). iPrMgCl·LiCl (1.3 M in THF, 1.07 mL, 1.39 mmol, 31 equiv.) was added dropwise and the solution was stirred for 1 h resulting in a yellow solution. Ni(*o*-tolyl)(dppe)Cl (27 mg, 0.046 mmol, 1 equiv.) was dissolved in dry THF (2 mL) and injected quickly into the 1,4-dibromo-2,5-bis(2-ethylhexyloxy)benzene solution causing a deep yellow color to immediately evolve. This was stirred for 40 min and after such time a small aliquot (1.5 mL) was removed from the flask and quenched with 5M HCl prior to analysis by GPC. The thiophene monomer solution was injected quickly into the 1,4-dibromo-2,5-bis(2-ethylhexyloxy)benzene solution causing a dark orange color to evolve. The solution was stirred for 30 min., a septum was affixed, the flask was removed from the glove box and then quenched using 5M HCl (12 mL) followed by stirring for an additional 15 min. $CHCl_3$ (100 mL) was added, the solution was washed using distilled water (3 x 100 mL), dried using $MgSO_4$, gravity filtered and then concentrated *in vacuo* to yield a reddish-purple solid. The crude product was dissolved in $CHCl_3$ and precipitated into ice-cold

MeOH followed by acetone which yielded a reddish-purple solid. The crude solid was purified further using preparatory GPC with THF as the eluent (380 mg, 69% yield).

$^1$H NMR (500 MHz, $CDCl_3$) (ppm): 7.44 (d, 2H, phenyl-H, **Ha**), 7.17 (d, 2H, phenyl-H, **Hb**) 7.08-7.04 (bs, 30H, phenylene-H, **Hc**), 7.00-6.97 (bs, 35H, thiophene-H, **Hd**) 3.80-3.71 (bm, 60H, phenylene-O-$CH_2$-CH, **He**), 2.84-2.79 (bt, 70H, thiophene-$CH_2$-$C_5H_{11}$, **Hf**) 2.25 (s, 3H, *o*-tolyl-$CH_3$, **Hg**) 1.76-1.68 (bm, 30H, O-$CH_2$-CH, **Hh**), 1.47-1.20 (m, 520H, -$CH_2$-, **Hi**) 0.95-0.90 (bt, 105H, thiophene-$C_5H_{10}$-$CH_3$, **Hj**), 0.87-0.80 (bm, 180H, O-$C_3H_5$-$CH_3$ and O-$C_5H_9$-$CH_3$, **Hk**)

Diblock Copolymer: GPC: $M_n$ = 12, 000 Da, $Đ_M$ = 1.08

Work-up of $PPP_{15}$ homopolymer aliquot: $CHCl_3$ (25 mL) was added to the 5M HCl solution and the mixture was washed using distilled water (3 x 50 mL). The organic phase was dried over $MgSO_4$, gravity filtered, and concentrated *in vacuo* to a yellow oil. MeOH (50 mL) was added, and the solution was shaken vigorously and sonicated using a sonication bath. The yellow solid was collected by vacuum filtration and washed thoroughly with MeOH to yield the homopolymer as a yellow, gum-like residue.

PPP Homopolymer: GPC: $M_n$ = 5, 500 Da, $Đ_M$ = 1.14, $DP_{n,\,GPC}$ = 17; $DP_{n,\,H\,NMR}$ = 15

$^1$H NMR (500 MHz, $CDCl_3$) (ppm): 7.44 (d, 2H, phenyl-H, **Ha**), 7.17 (d, 2H, phenyl-H, **Hb**) 7.08-7.00 (bs, 2H, phenylene-H, **Hc**) 3.85-3.68 (bm, 4H, phenylene-O-$CH_2$-CH, **Hd**), 2.25 (s, o-tolyl-$CH_3$, **He**) 1.80-1.70 (m, 2H, O-$CH_2$-CH, **Hf**), 1.40-1.07 (m, 16H, -$CH_2$-, **Hg**) 0.90-0.79 (bm, 12H, -$CH_3$, **Hh**)

**Scheme S3. Synthesis of P3HT$_{60}$-*b*-PPP$_{30}$**

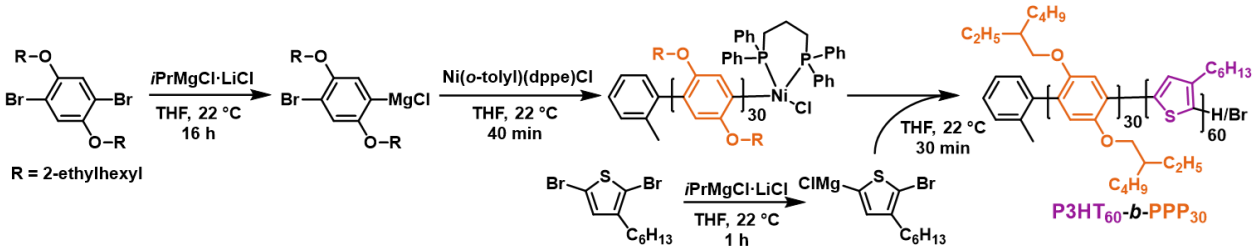


The synthesis of **P3HT$_{60}$-*b*-PPP$_{30}$** was carried out using the same procedure for **P3HT$_{35}$-*b*-PPP$_{15}$** detailed above. (180 mg, 38% yield).

Diblock Copolymer: GPC: $M_n$ = 18, 200 Da, $Đ_M$ = 1.10

$^1$H NMR (500 MHz, $CDCl_3$) (ppm): 7.44 (d, 2H, phenyl-H, **Ha**), 7.17 (d, 2H, phenyl-H, **Hb**) 7.08-7.04 (bs, 60H, phenylene-H, **Hc**), 7.00-6-97 (bs, 60H, thiophene-H, **Hd**) 3.80-3.71 (bm, 120H, phenylene-O-$CH_2$-CH, **He**), 2.84-2.79 (bt, 120H, thiophene-$CH_2$-$C_5H_{11}$, **Hf**) 2.25 (s, 3H, *o*-tolyl-$CH_3$, **Hg**) 1.76-1.68 (bm, 60H, O-$CH_2$-CH, **Hh**), 1.47-1.20 (m, 960H, -$CH_2$-, **Hi**) 0.95-0.90 (bt, 180H, thiophene-$C_5H_{10}$-$CH_3$, **Hj**), 0.87-0.80 (bm, 360H, O-$C_3H_5$-$CH_3$ and O-$C_5H_9$-$CH_3$, **Hk**)

$PPP_{30}$ Homopolymer: GPC: $M_n$ = 10, 800 Da, $Đ_M$ = 1.11, $DP_{n,\ GPC}$ = 32; $DP_{n,\ H\ NMR}$ = 30

$^1$H NMR (500 MHz, $CDCl_3$) (ppm): 7.36 (d, 2H, phenyl-H, **Ha**), 7.12 (d, 2H, phenyl-H, **Hb**) 7.08-7.00 (bs, 60H, phenyl-H, **Hc**) 3.85-3.68 (bm, 4H, phenyl-O-$CH_2$-CH, **Hd**), 2.25 (s, *o*-tolyl-$CH_3$, **He**) 1.65-1.57 (m, 60H, O-$CH_2$-CH, **Hf**), 1.40-1.07 (m, 480H, -$CH_2$-, **Hg**) 0.90-0.79 (bm, 12H, -$CH_3$, **Hh**).

## Structural Characterization of P3HT$_{60}$-*b*-PPP$_{30}$ and P3HT$_{35}$-*b*-PPP$_{15}$

### Gel Permeation Chromatography

#### P3HT$_{60}$-*b*-PPP$_{30}$

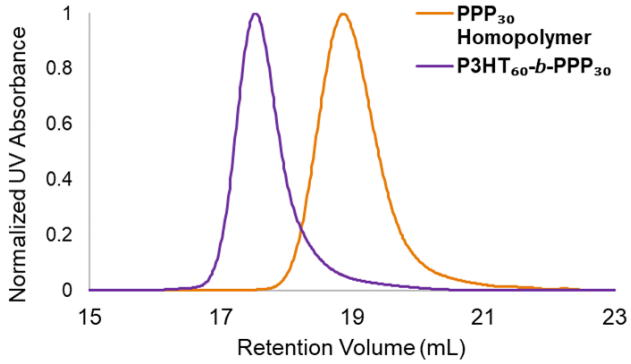


**Figure S1.** Overlaid GPC chromatograms of P3HT$_{60}$-*b*-PPP$_{30}$ BCP (purple trace) and its corresponding coronal-block PPP$_{30}$ homopolymer (orange trace) using UV/Vis detection at an absorbance wavelength of 330 nm.

#### P3HT$_{35}$-*b*-PPP$_{15}$

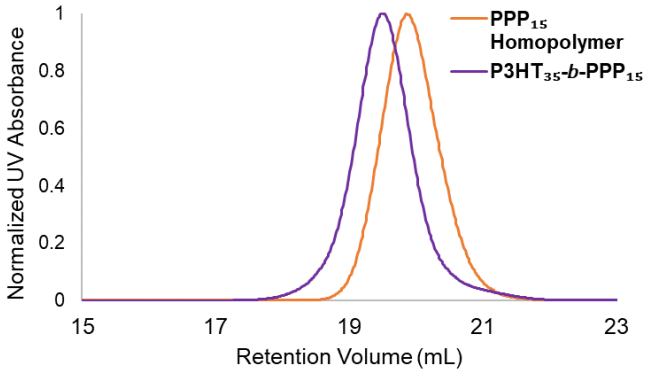


**Figure S2.** Overlaid GPC chromatograms of P3HT$_{35}$-*b*-PPP$_{15}$ BCP (purple trace) and its corresponding coronal-block PPP$_{15}$ homopolymer (orange trace) using UV/Vis detection at an absorbance wavelength of 330 nm.

**Differential Scanning Calorimetry**

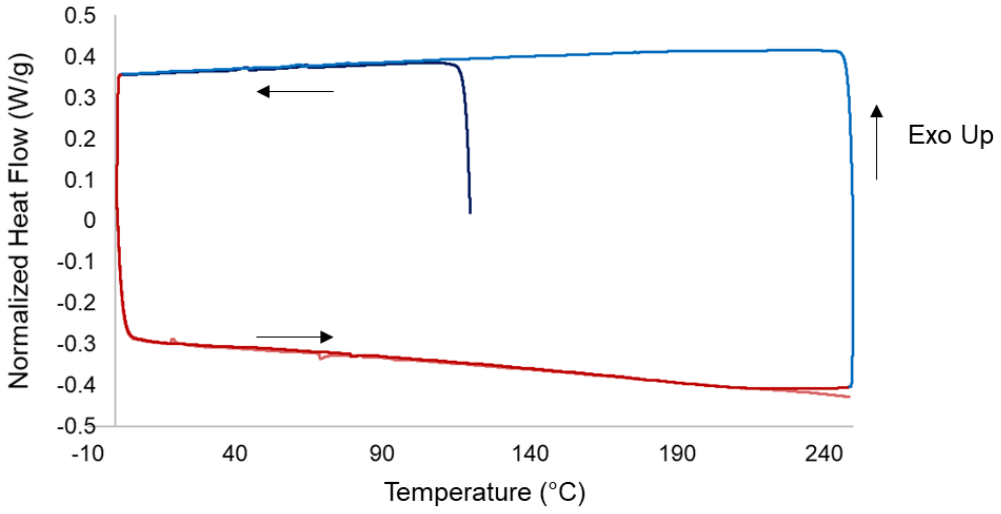


**Figure S3.** DSC thermogram of $PPP_{30}$ heated at a temperature ramp rate of 10 °C/min under $N_2$ showing no $T_c$ or $T_m$. Arrows denote the direction of heating and cooling cycles. The thermal history of the material was removed by annealing at 120 °C for 3 h under $N_2$ flow prior to being subjected to two cool-heat cycles from 0 °C to 250 °C, at a temperature ramp rate of 10 °C/min. 120 °C was chosen as the annealing temperature as this is ~25 °C above the reported $T_m$ of PPP homopolymer.[5]

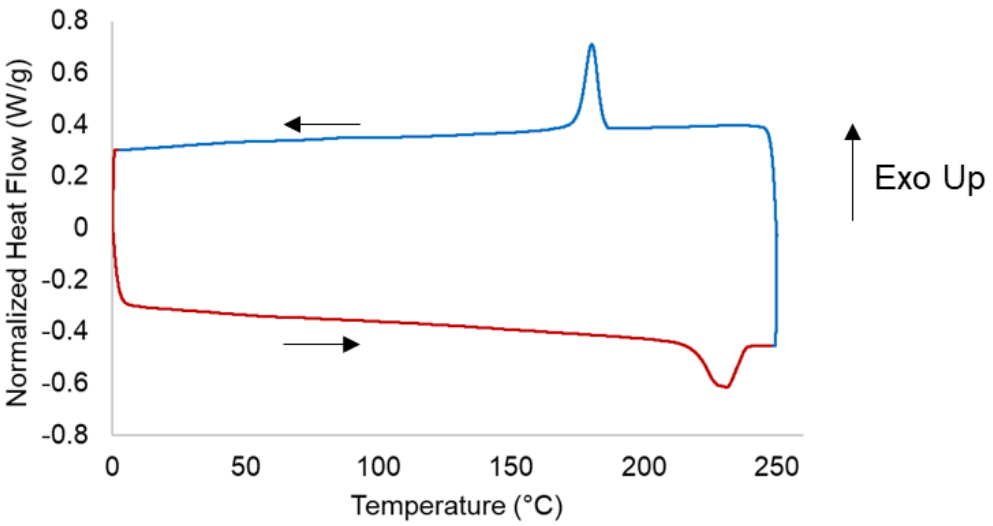


**Figure S4.** DSC thermogram of P3HT$_{60}$-*b*-PPP$_{30}$ heated at a temperature ramp rate of 10 °C/min under $N_2$. Arrows denote the direction of heating and cooling cycles. $T_m$ peak temperature = 231 °C with a melting enthalpy of 13.0 J/g. $T_c$ = 180 °C with an enthalpy of crystallization of 12.0 J/g.

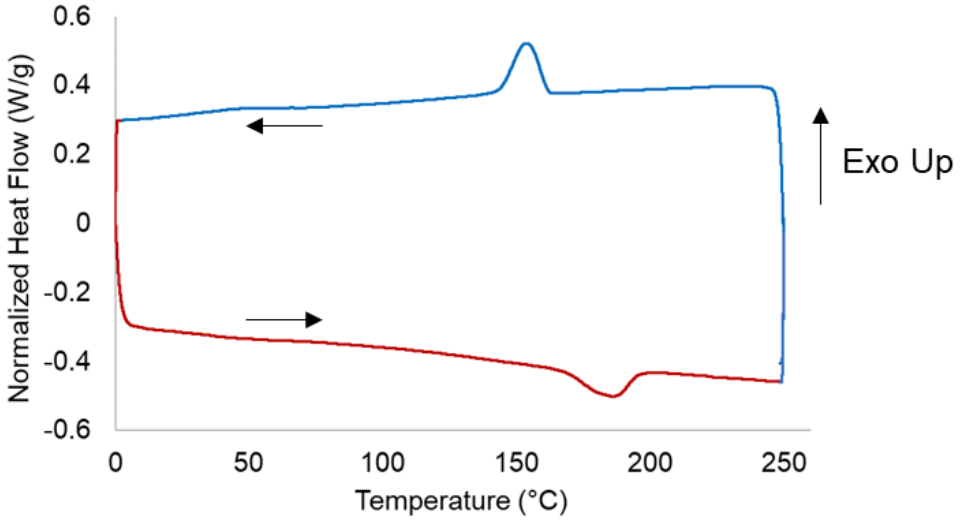


**Figure S5.** DSC thermogram of P3HT$_{35}$-*b*-PPP$_{15}$ heated at a temperature ramp rate of 10 °C/min under $N_2$. Arrows denote the direction of heating and cooling cycles. $T_m$ peak temperature = 186 °C with a melting enthalpy of 8.2 J/g. $T_c$ = 153 °C with an enthalpy of crystallization of 9.9 J/g.

## $^1$H NMR Spectroscopy

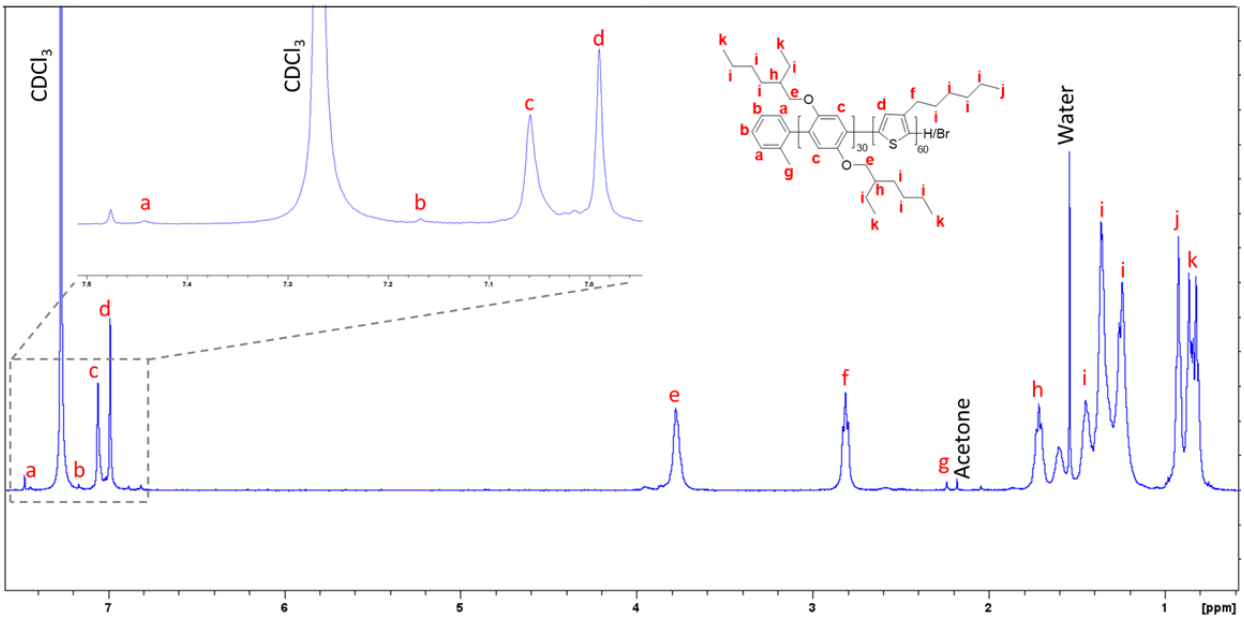


**Figure S6.** $^1$H NMR spectrum of P3HT$_{60}$-*b*-PPP$_{30}$ (500 MHz, $CDCl_3$).

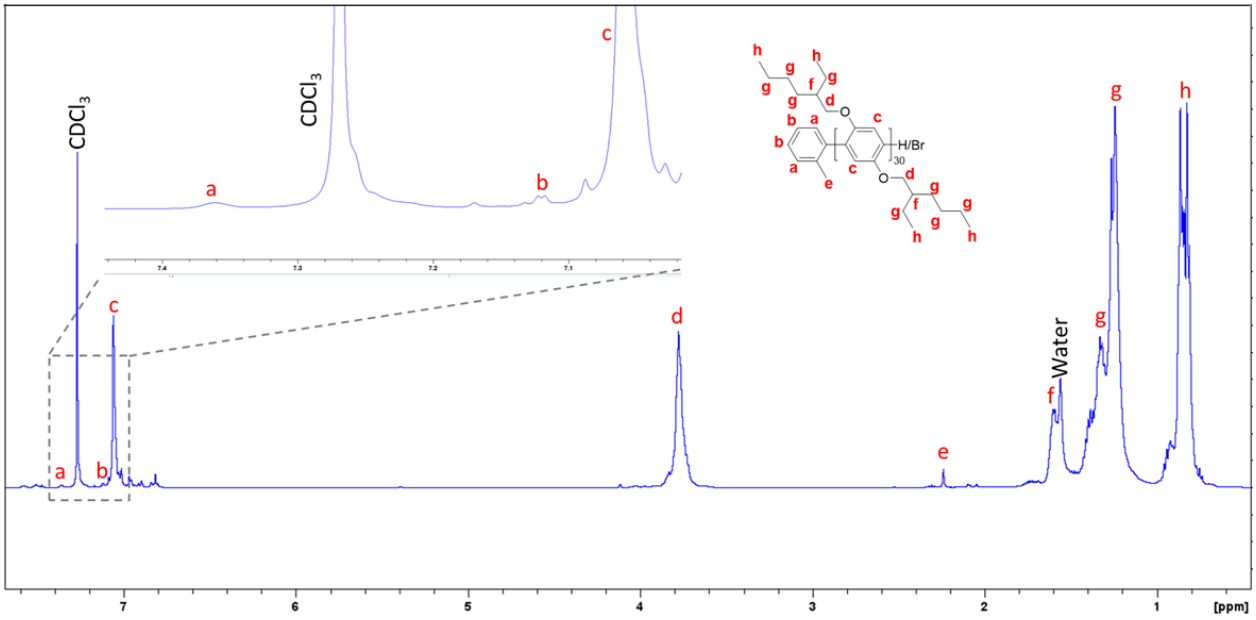


**Figure S7.** $^1$H NMR spectrum of PPP$_{30}$ homopolymer (500 MHz, $CDCl_3$).

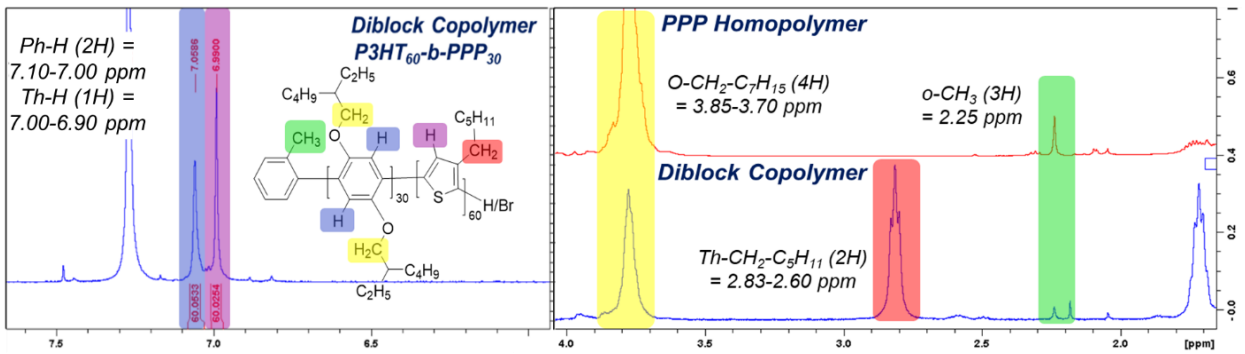


**Figure S8.** $^{1}$H NMR spectra of $PPP_{30}$ homopolymer and $P3HT_{60}$-*b*-$PPP_{30}$ in $CDCl_3$ highlighting how relative integrations are used to determine degree of polymerization. The spectrum exhibits a small singlet at 2.25 ppm corresponding to the *ortho*-tolyl methyl group. The spectrum exhibits a singlet corresponding to the two protons in the 3- and 6- positions on the phenyl rings (denoted in blue) that can be used for relative integration; however, this signal can overlap with the singlet peak from 7.00-6.90 ppm corresponding to the vinylic proton in the 4- position on the thiophene rings (denoted in purple). The vinylic proton signal can be used to determine the P3HT core-block $DP_n$ which was found to be 60 in this example. In the case of overlap between the two signals around 7.00 ppm, the broad signal from 3.85-3.70 ppm (denoted in yellow) corresponding to the methylene protons adjacent to the oxygen atoms at the 2- and 5- positions on the phenyl rings can be used. The relative integration ratio of this signal to the *o*-tolyl methyl resonance was 120:3, giving a $DP_n$ of the PPP block of 30.

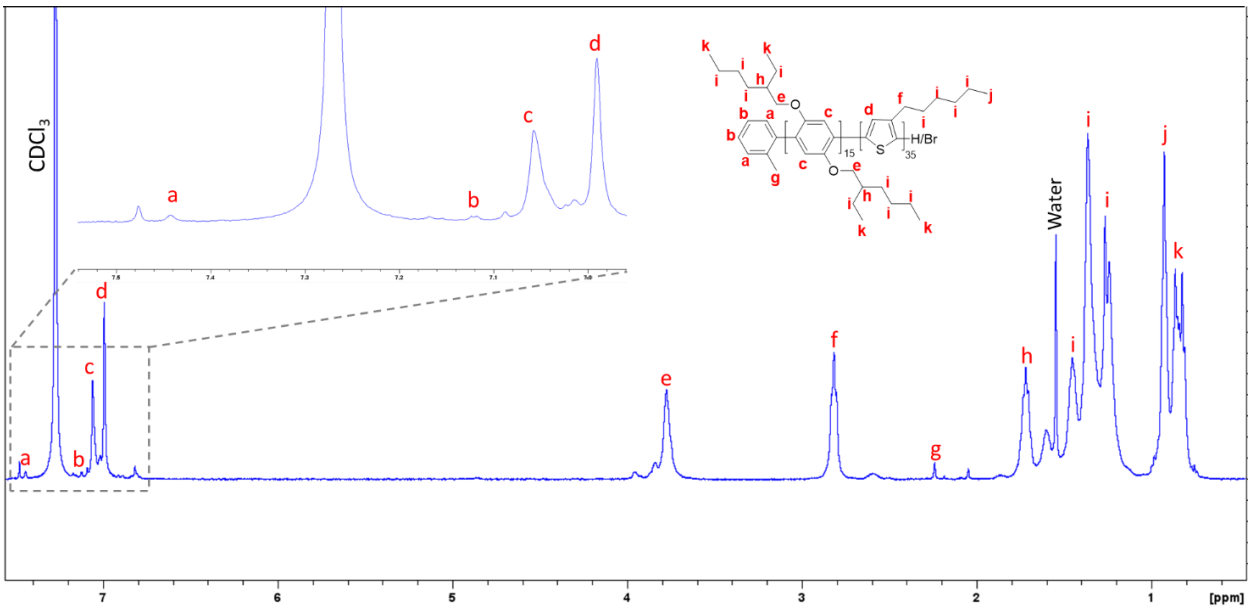


**Figure S9.** $^{1}$H NMR spectrum of P3HT$_{35}$-*b*-PPP$_{15}$ (500 MHz, $CDCl_3$).

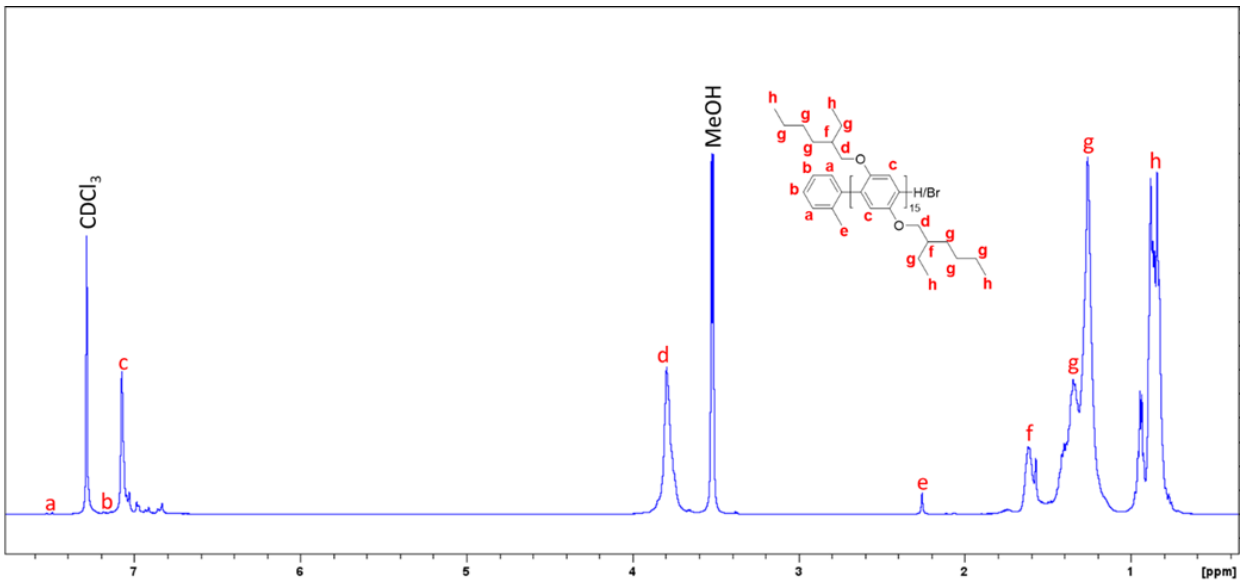


**Figure S10.** $^{1}$H NMR spectrum of PPP$_{15}$ homopolymer (500 MHz, $CDCl_3$).

## Crystallization-Driven Self-Assembly

### General self-assembly procedure for fabrication of polydisperse fibers and seed micelles

#### P3HT$_{60}$-*b*-PPP$_{30}$

Self-assembly of P3HT$_{60}$-*b*-PPP$_{30}$ into polydisperse fiber-like micelles was achieved by adding 4 mL of *n*BuAc to a vial containing 4 mg of P3HT$_{60}$-*b*-PPP$_{30}$ (1 mg/mL). The vial was then placed in a metal heating block at 80 °C and heated for 30 min. The 1 mg/mL solution was allowed to cool to 22 °C slowly (ca. 4 h) followed by aging for 24 h. The vial was then placed in a 0 °C ultrasonic cleaning bath and sonicated for 4 h to give seed micelles (37 kHz, 100% power). Seeds were then annealed at 30 °C for 18 h prior to use.

#### P3HT$_{35}$-*b*-PPP$_{15}$

Self-assembly of P3HT$_{35}$-*b*-PPP$_{15}$ into polydisperse fiber-like micelles was achieved by adding 4 mL of *n*BuAc to a vial containing 4 mg of P3HT$_{35}$-*b*-PPP$_{15}$ (1 mg/mL). The vial was then placed in a metal heating block at 90 °C and heated for 30 min. The 1 mg/mL solution was allowed to cool to 22 °C slowly (ca. 4 h) followed by aging for 24 h. A sonotrode affixed with a titanium probe was placed in an *n*BuAc solution (1 mg/mL) of polydisperse P3HT$_{35}$-*b*-PPP$_{15}$ micelles at -45 °C and sonicated for 7 h at 100% power. Seeds were then annealed at 30 °C for 18 h prior to use.

### General self-assembly procedure for attempted length-control of P3HT$_{35}$-*b*-PPP$_{15}$ nanofibers *via* seeded growth at 22 °C

P3HT$_{35}$-*b*-PPP$_{15}$ seed micelle solution (*n*BuAc, 0.1 mg/mL) was added to a vial and diluted with *n*BuAc such that the final concentration will be 0.05 mg/mL following unimer addition. P3HT$_{35}$-*b*-PPP$_{15}$ unimer solution (1 mg/mL in THF) was added quickly, the solutions were vortexed for

10 s and then aged at 22 °C for 24 h prior to imaging by TEM.

**General self-assembly procedure for attempted length-control of P3HT$_{35}$-*b*-PPP$_{15}$ nanofibers *via* self-nucleation suppressed seeded growth at 50 °C**

Four vials were filled with increasing amounts of polydisperse P3HT$_{35}$-*b*-PPP$_{15}$ nanofiber solution (*n*BuAc, 0.1 mg/mL) and diluted using *n*BuAc such that the final concentration after seed addition will be 0.05 mg/mL. The solutions were heated to 90 °C for 1 h and then cooled to 50 °C over ~2 h by placing in a preheated metal block. Equal amounts of seed micelle solution at 50 °C (*n*BuAc, 0.1 mg/mL) correlating to $m_{unimer}/m_{seed}$ = 1, 2, 3, and 4 were added quickly, the solutions were vortexed for 10 s and then placed back in the 50 °C heating block for 24 h before cooling to 22 °C slowly (ca. 2 h) and aged 24 h prior to imaging by TEM.

**Atomic Force Microscopy**

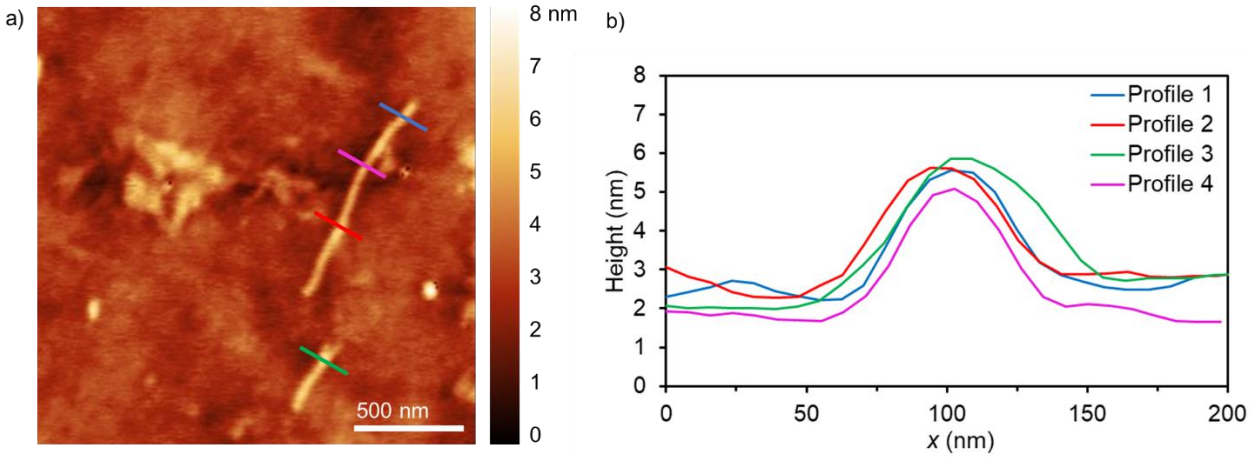


**Figure S11. (a)** AFM height image of polydisperse P3HT$_{60}$-*b*-PPP$_{30}$ nanofibers in *n*BuAc (0.05 mg/mL) drop-cast onto a glow discharged silicon wafer. Coloured lines indicate height profile shown in **(b)** drawn perpendicular to the long axis of the fibers. Series 1 - height: 3.32 nm, width: 93.67 nm; Series 2 - height: 3.32 nm, width: 93.97 nm; Series 3 - height: 3.38 nm, width: 101.14

nm; Series 4 - height: 3.43 nm, width: 89.89 nm. Average height: 3.49 nm ± 0.27 nm. Average width: ($W_n$ = 94.67 nm ± 4.7 nm).

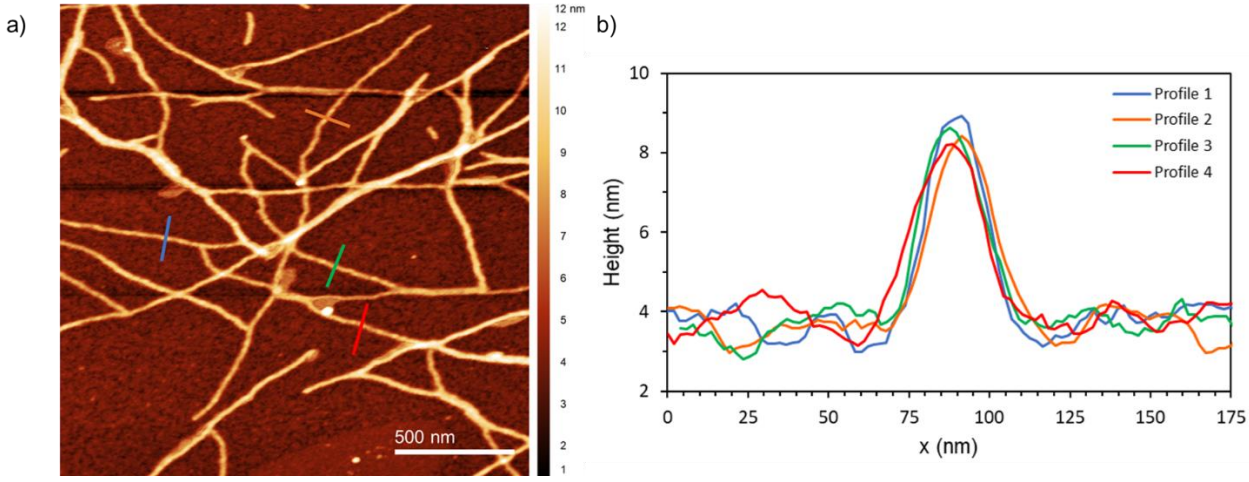


**Figure S12. (a)** AFM height image of polydisperse P3HT$_{35}$-*b*-PPP$_{15}$ nanofibers in *n*BuAc (0.05 mg/mL) drop-cast onto a glow discharged silicon wafer. Coloured lines indicate height profile shown in **(b)** drawn perpendicular to the long axis of the fibers. Series 1 - height: 5.73 nm, width: 48.52 nm; Series 2 - height: 5.21 nm, width: 52.5 nm; Series 3 - height: 5.42 nm, width: 45.2 nm; Series 4 - height: 5.02 nm, width: 52.6 nm. Average height: 5.35 nm ± 0.26 nm. Average width: ($W_n$ = 49.70 nm ± 3.1 nm).

**Variable Temperature UV/Vis Spectroscopy**

**P3HT$_{35}$-*b*-PPP$_{15}$**

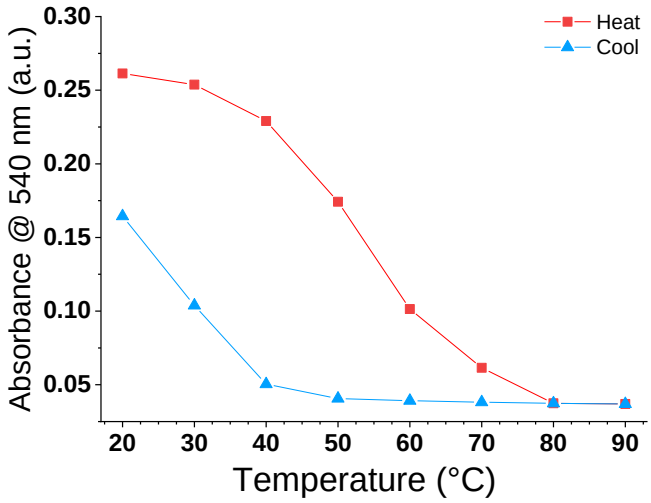


**Figure S13.** Absorbance plot showing a thermal hysteresis during heating and cooling of a *n*BuAc P3HT$_{35}$-*b*-PPP$_{15}$ polydisperse micelle solution (0.05 mg/mL) heated from 20 °C to 90 °C and then cooled from 90 °C back to 20 °C using 10 °C increments at a rate of 10 °C/min. Solutions were allowed to equilibrate at the target temperatures for 30 min. prior to each scan being taken. Absorbance wavelength chosen to monitor solution was 540 nm. Upon cooling, it was found that the absorbance peak at 540 nm became visible below 50 °C suggesting that above this temperature, nucleation had not yet occurred or was occurring at a very slow rate. This behavior has been observed in other P3HT-based systems, due to the crystal lattice energy that needs to be overcome for dissolution to occur.[6,7]

## Nanofiber Characterization by TEM

### Polydisperse Micelles

#### P3HT$_{60}$-*b*-PPP$_{30}$

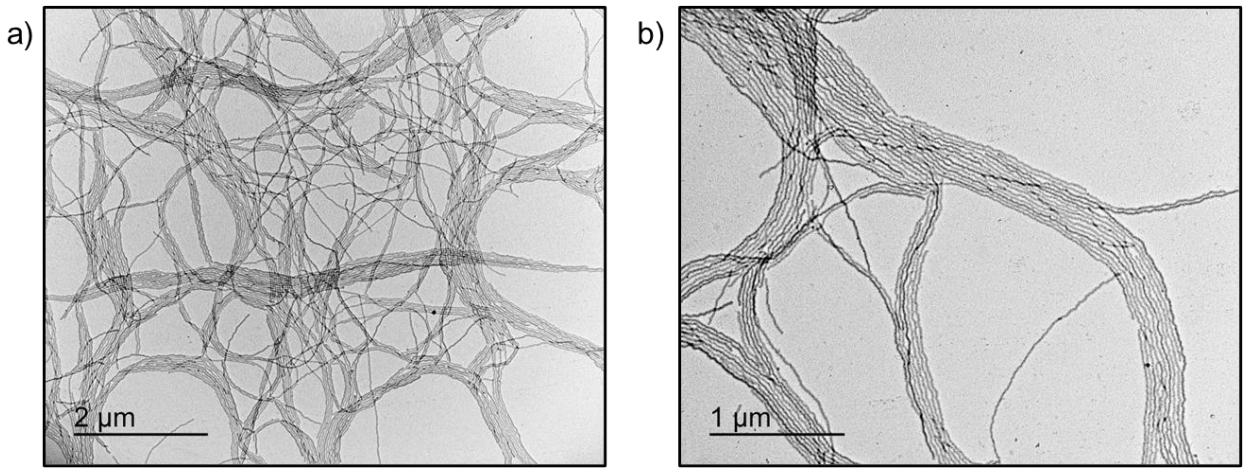


**Figure S14. (a, b)** TEM images of polydisperse P3HT$_{60}$-*b*-PPP$_{30}$ fibers made by heating solid P3HT$_{60}$-*b*-PPP$_{30}$ in *n*BuAc to 80 °C for 30 min. and cooling the solution (1 mg/mL) to 22 °C followed by aging for 24 h. The samples were then drop-cast onto a carbon-coated copper TEM grid and imaged following solvent evaporation. Width analysis of polydisperse fiber-like micelles that were imaged using TEM showed that $W_n$ was 21.8 ± 5.7 nm (number counted = 8).

**P3HT$_{35}$-*b*-PPP$_{15}$**

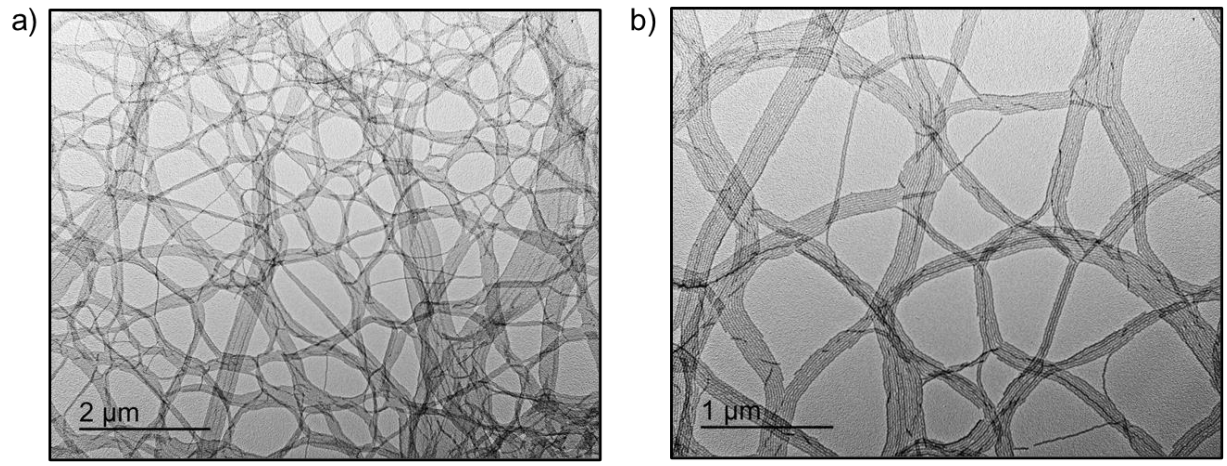


**Figure S15. (a, b)** TEM images of polydisperse P3HT$_{35}$-*b*-PPP$_{15}$ fibers made by heating solid P3HT$_{35}$-*b*-PPP$_{15}$ in *n*BuAc to 80 °C for 30 min. and cooling the solution (1 mg/mL) to 22 °C followed by aging for 24 h. The samples were then drop-cast onto a carbon-coated copper TEM grid and imaged following solvent evaporation. Width analysis of polydisperse fiber-like micelles that were imaged using TEM showed that the $W_n$ was 12.7 ± 2.4 nm (number counted = 8).

**Seed Fabrication**

**P3HT$_{60}$-*b*-PPP$_{30}$ - Sonication Bath**

**Not Annealed**

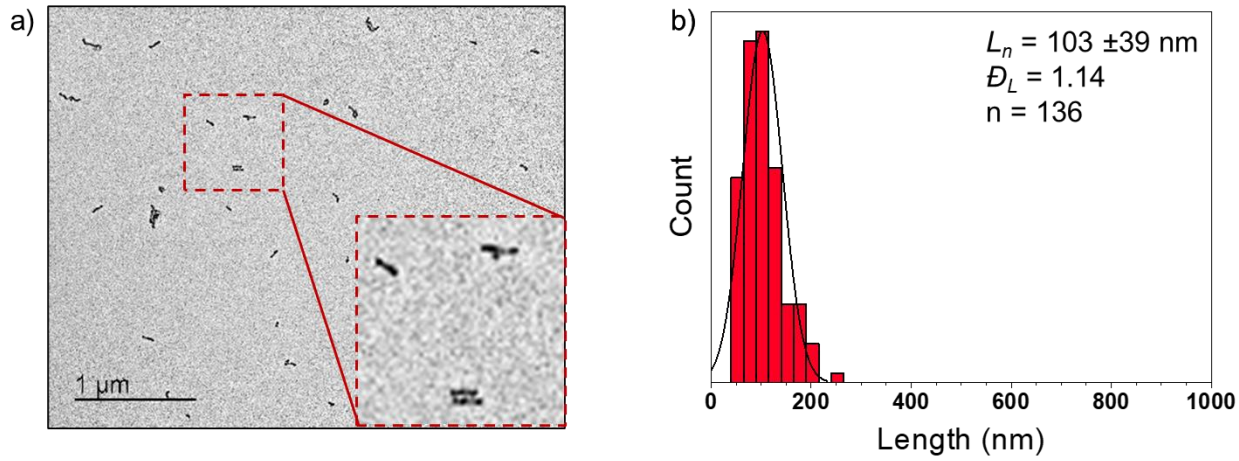


**Figure S16. (a)** TEM image of seeds formed by ultrasonication of a P3HT$_{60}$-*b*-PPP$_{30}$ polydisperse micelle solution (*n*BuAc, 1 mg/mL) in a 0 °C bath for 4 h (37 kHz, 100% power). **(b)** Histogram showing the fiber length distribution of P3HT$_{60}$-*b*-PPP$_{30}$ seeds ($L_n$ = 103 nm, $L_w$ = 118 nm, $Đ_L$ = 1.14, σ = ± 39 nm, n = 136).

**Annealed at 30 °C**

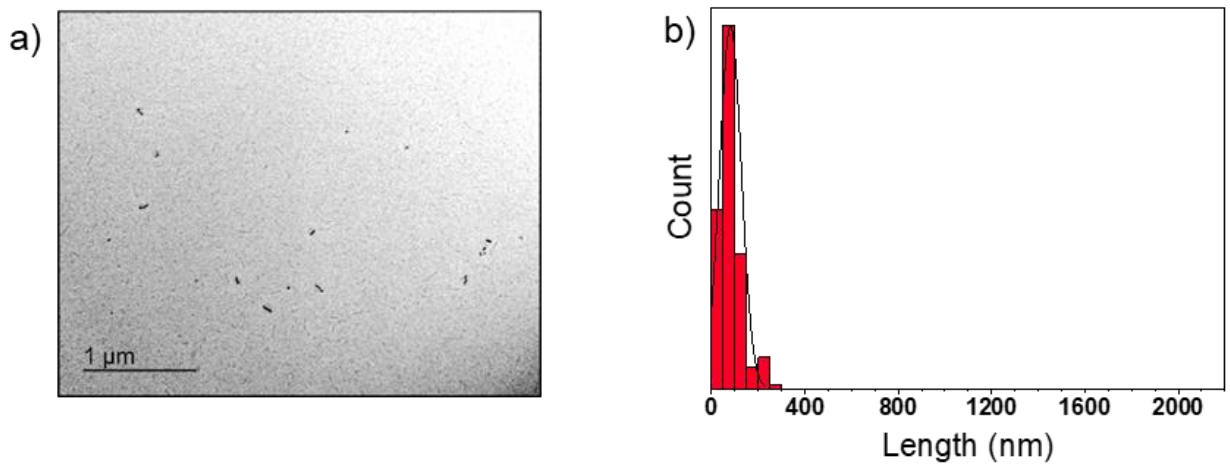


**Figure S17.** **(a)** TEM image of P3HT$_{60}$-*b*-PPP$_{30}$ seeds that were diluted to 0.1 mg/mL using *n*BuAc and annealed for 18 h at 30 °C before being brought to 22 °C (ca. 2 h). **(b)** Histogram showing the fiber length distribution of P3HT$_{60}$-*b*-PPP$_{30}$ seeds ($L_n$ = 81 nm, $L_w$ = 108 nm, $Đ_L$ = 1.33, σ = ± 47 nm, n = 163).

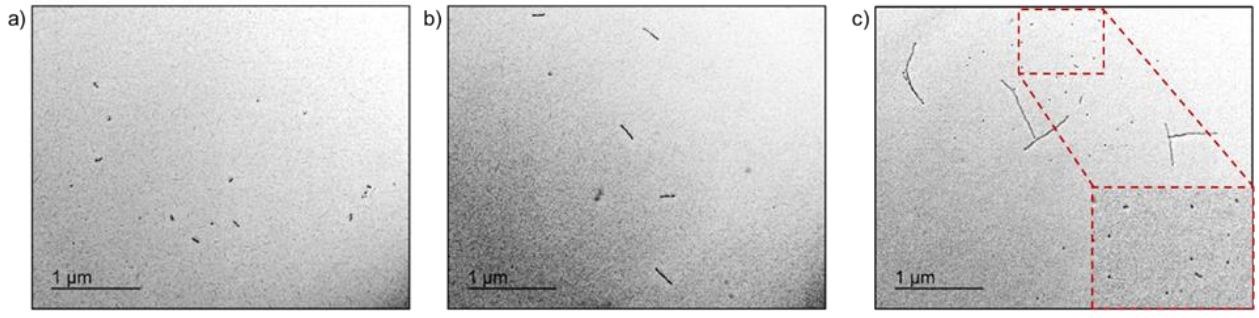


**Figure S18.** TEM images of P3HT$_{60}$-*b*-PPP$_{30}$ seeds that were diluted to 0.1 mg/mL using *n*BuAc and annealed at **(a)** 30 °C, **(b)** 35 °C and **(c)** 40 °C for 18 h at before being brought to 22 °C and aged at 22 °C for 24 h. **(c)** Inset shows small nanofiber fragments amongst elongated fibers.

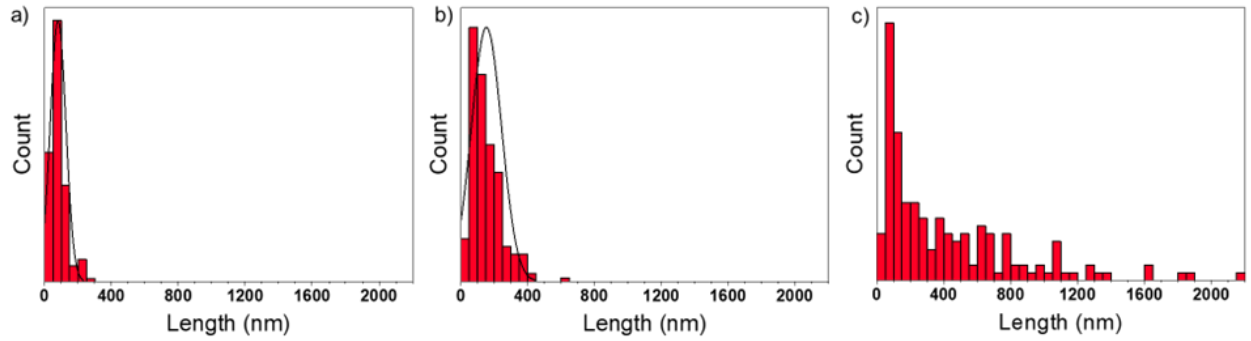


**Figure S19.** Histograms showing P3HT$_{60}$-*b*-PPP$_{30}$ nanofiber contour length distributions after annealing seeds at **(a)** 30 °C, **(b)** 35 °C and **(c)** 40 °C for 18 h and then cooled to 22 °C and aged at 22 °C for 24 h. **(a)** 30 °C: $L_n$ = 81 nm, $Đ_L$ = 1.33, σ = ± 47. **(b)** 35 °C: $L_n$ = 153 nm, $Đ_L$ = 1.35, σ = ± 90). **(c)** 40 °C: $L_n$ = 417 nm, $Đ_L$ = 1.98, σ = ± 412.

**P3HT$_{35}$-*b*-PPP$_{15}$ – Sonication Bath**

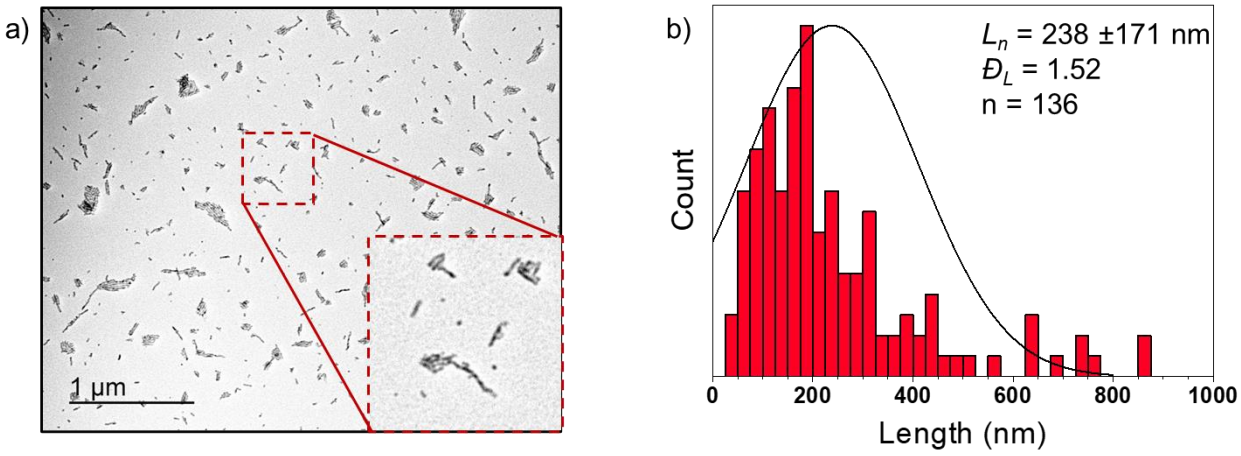


**Figure S20. (a)** TEM image of seeds formed from ultrasonication of a P3HT$_{35}$-*b*-PPP$_{15}$ polydisperse nanofiber solution (*n*BuAc, 1 mg/mL) in a 0 °C bath for 7 h (100% power). **(b)** Histogram showing the fiber length distribution of P3HT$_{35}$-*b*-PPP$_{15}$ seeds ($L_n$ = 238 nm, $L_w$ = 362 nm, $Đ_L$ = 1.52, σ = ± 171 nm, n = 136).

**P3HT$_{35}$-*b*-PPP$_{15}$ – Sonotrode Probe**

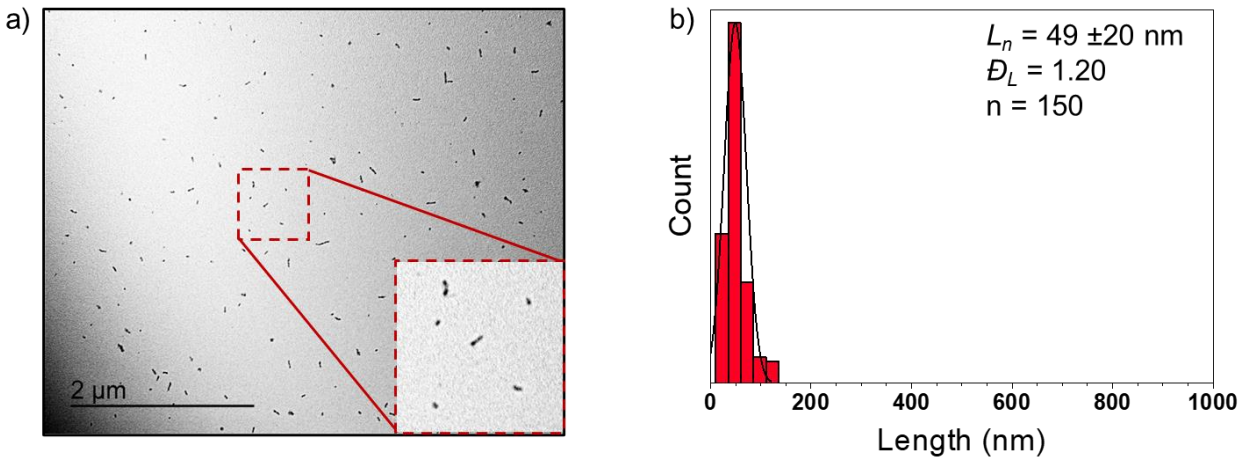


**Figure S21. (a)** TEM image of seeds formed from ultrasonication of a P3HT$_{35}$-*b*-PPP$_{15}$ polydisperse nanofiber solution (*n*BuAc, 1 mg/mL) at -45 °C using a sonotrode probe for 7 h (100% power). Seeds were annealed at 30 °C for 18 h prior to use. **(b)** Histogram showing the fiber length distribution of P3HT$_{35}$-*b*-PPP$_{15}$ seeds ($L_n$ = 49 nm, $L_w$ = 59 nm, $Đ_L$ = 1.20, σ = ± 20 nm, n = 150).

**Attempted seeded growth of length-controlled P3HT$_{60}$-*b*-PPP$_{30}$ nanofibers at 22 °C using annealed seeds**

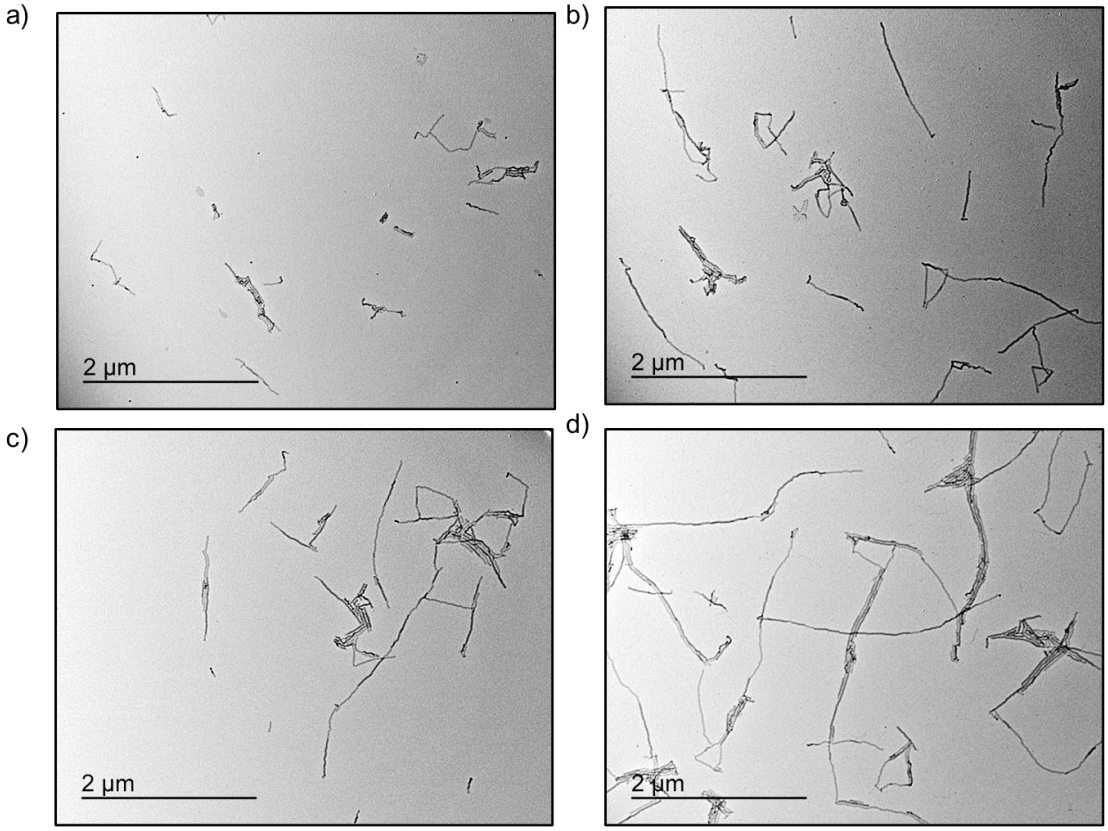


**Figure S22.** TEM images of P3HT$_{60}$-*b*-PPP$_{30}$ nanofibers in (*n*BuAc, 0.05 mg/mL) formed by living CDSA seeded growth using addition of **(a)** 1, **(b)** 2, **(c)** 3, and **(d)** 4 equivalents of P3HT$_{60}$-*b*-PPP$_{30}$ unimer solution (THF, 1 mg/mL) to P3HT$_{60}$-*b*-PPP$_{30}$ seeds (annealed, 30 °C, *n*BuAc, 0.1 mg/mL) at 22 °C. Solutions were aged at 22 °C for 24 h followed by solvent evaporation prior to TEM imaging.

**Attempted seeded growth of length-controlled P3HT$_{35}$-*b*-PPP$_{15}$ nanofibers at 22 °C using annealed seeds**

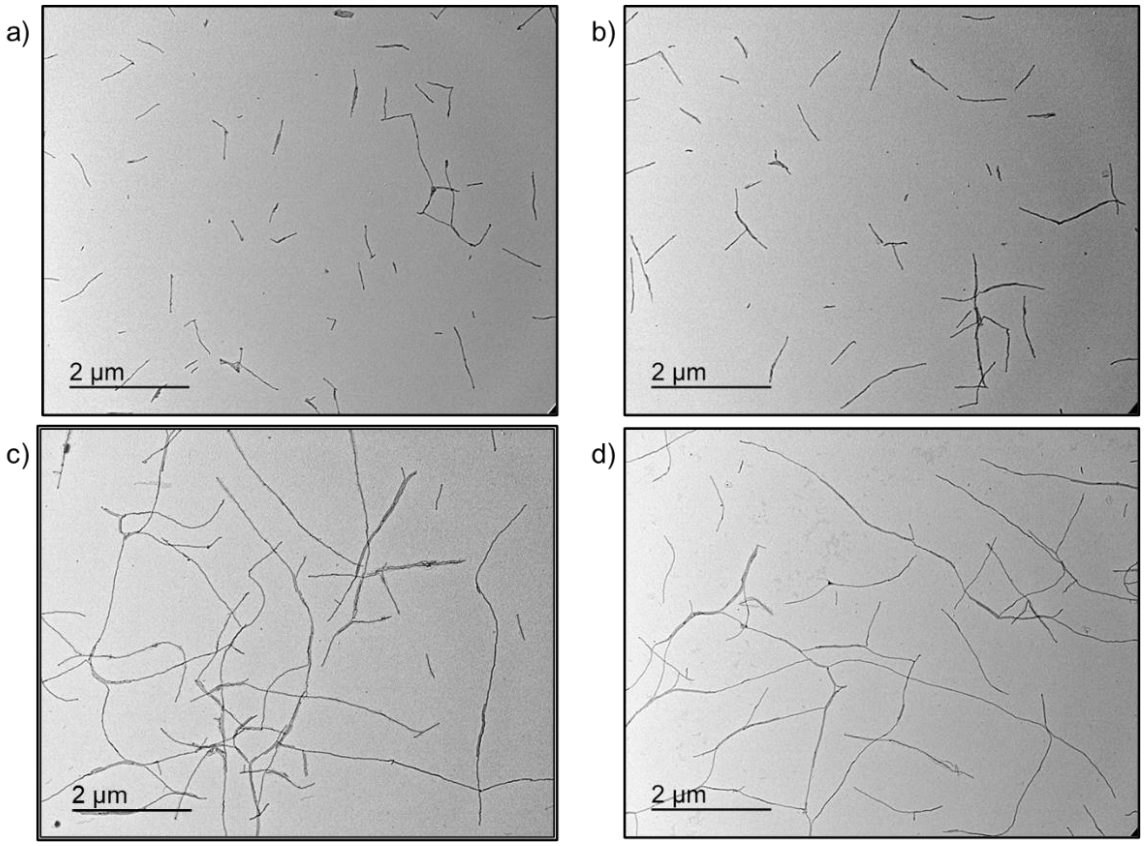


**Figure S23.** TEM images of P3HT$_{35}$-*b*-PPP$_{15}$ nanofibers in (*n*BuAc, 0.05 mg/mL) formed by living CDSA seeded growth using addition of **(a)** 1, **(b)** 2, **(c)** 3, and **(d)** 4 equivalents of P3HT$_{35}$-*b*-PPP$_{15}$ unimer solution (THF, 1 mg/mL) to P3HT$_{35}$-*b*-PPP$_{15}$ seed micelles (*n*BuAc, 0.1 mg/mL) at 22 °C. Solutions were aged at 22 °C for 24 h followed by solvent evaporation prior to TEM imaging.

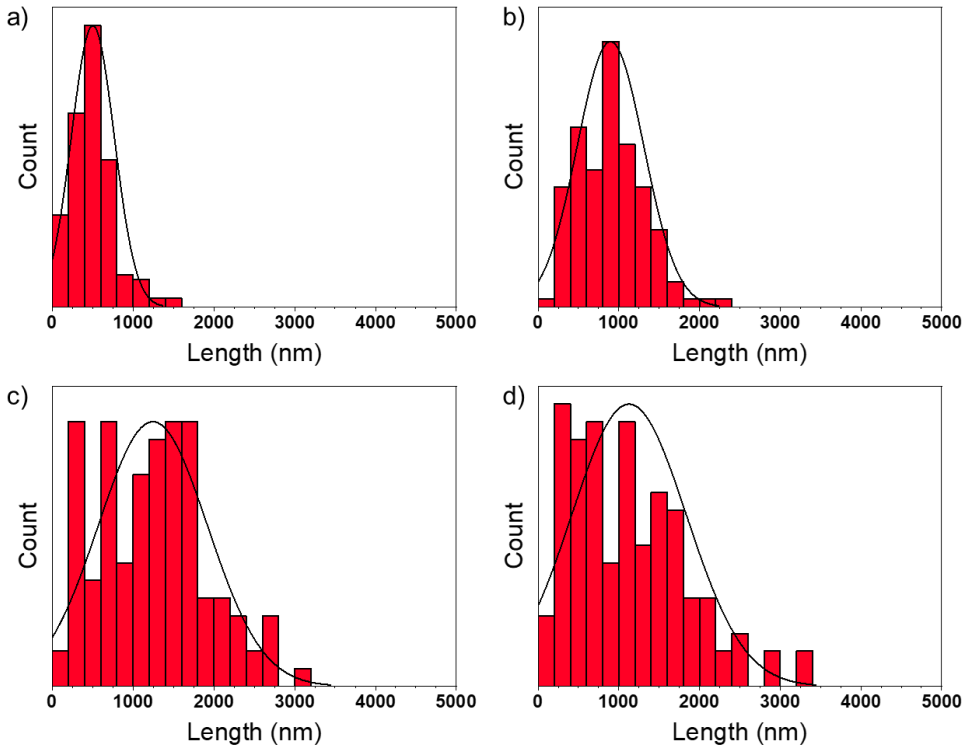


**Figure S24.** Histograms showing the nanofiber length distribution of P3HT$_{35}$-*b*-PPP$_{15}$ seed micelles (*n*BuAc, 0.1 mg/mL) that were treated with **(a)** 1, **(b)** 2, **(c)** 3, and **(d)** 4 equivalents of P3HT$_{35}$-*b*-PPP$_{15}$ unimer solution (1 mg/mL in THF) at 22 °C. Final concentrations were 0.05 mg/mL.

**Table S1. Summary of data from seeded growth experiments of homogeneous P3HT$_{35}$-*b*-PPP$_{15}$ nanofibers at 22 °C. σ is standard deviation in $L_n$ measurements.**

| $m_{unimer}/m_{seed}$ | $L_n$ | $L_w$ | $Đ_L$ | σ |
|---|---|---|---|---|
| Seeds | 49 | 59 | 1.20 | 22 |
| 1 | 502 | 636 | 1.27 | 265 |
| 2 | 896 | 1084 | 1.21 | 411 |
| 3 | 1261 | 1677 | 1.33 | 731 |
| 4 | 1126 | 1565 | 1.39 | 708 |

**Attempted self-nucleation suppressed seeded growth of P3HT$_{35}$-*b*-PPP$_{15}$ nanofibers at 50 °C**

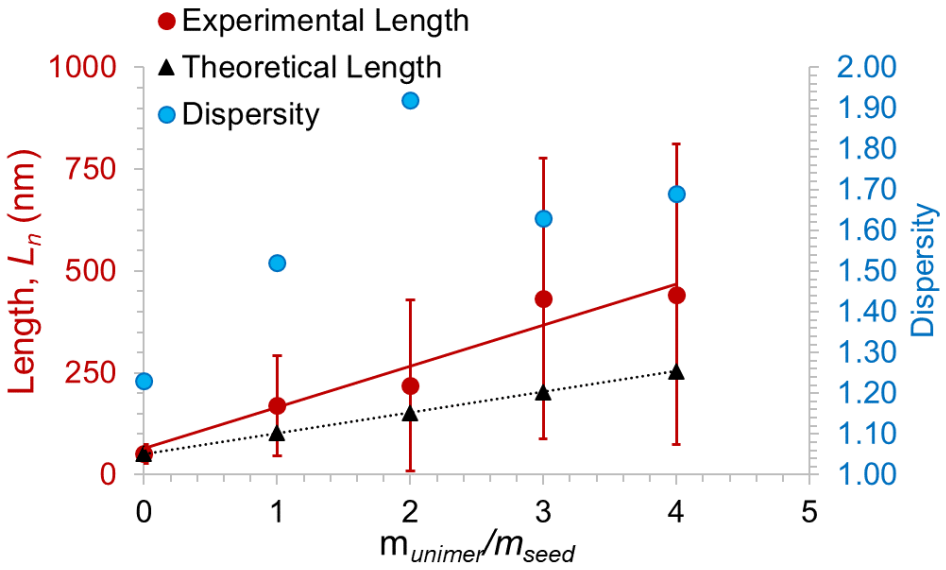


**Figure S25.** Plot showing the dependence of P3HT$_{35}$-*b*-PPP$_{15}$ nanofiber length ($L_n$) on unimer-to-seed ratio ($m_{unimer}/m_{seed}$) using self-nucleation suppressed seeded growth at 50 °C. Error bars represent standard deviation in $L_n$ measurements.

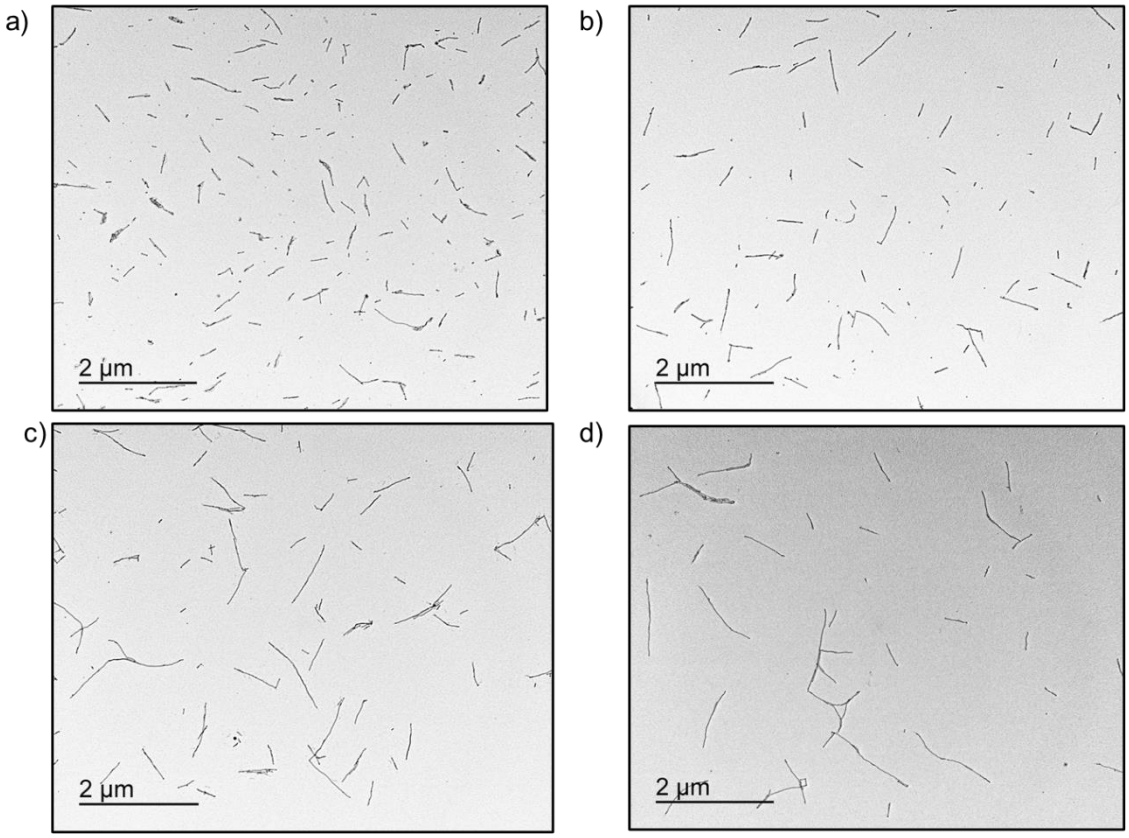


**Figure S26.** TEM images of P3HT$_{35}$-*b*-PPP$_{15}$ nanofibers in *n*BuAc (0.05 mg/mL) formed by self-nucleation suppressed seeded growth (50 °C) following solvent evaporation. Unimer-to-seed ratio $m_{unimer}/m_{seed}$ = **(a)** 1, **(b)** 2, **(c)** 3, and **(d)** 4. Fibers are formed through the addition of P3HT$_{35}$-*b*-PPP$_{15}$ seed micelles (*n*BuAc, 0.1 mg/mL) to polydisperse nanofiber solutions (*n*BuAc, 0.1 mg/mL) which were heated to 90 °C for 1 h and then cooled to 50 °C over the course of 2 h. Following seed addition at 50 °C, the solutions were maintained at 50 ° C for an additional 24 h before being cooled to 22 °C and aged at 22 °C for 24 h.

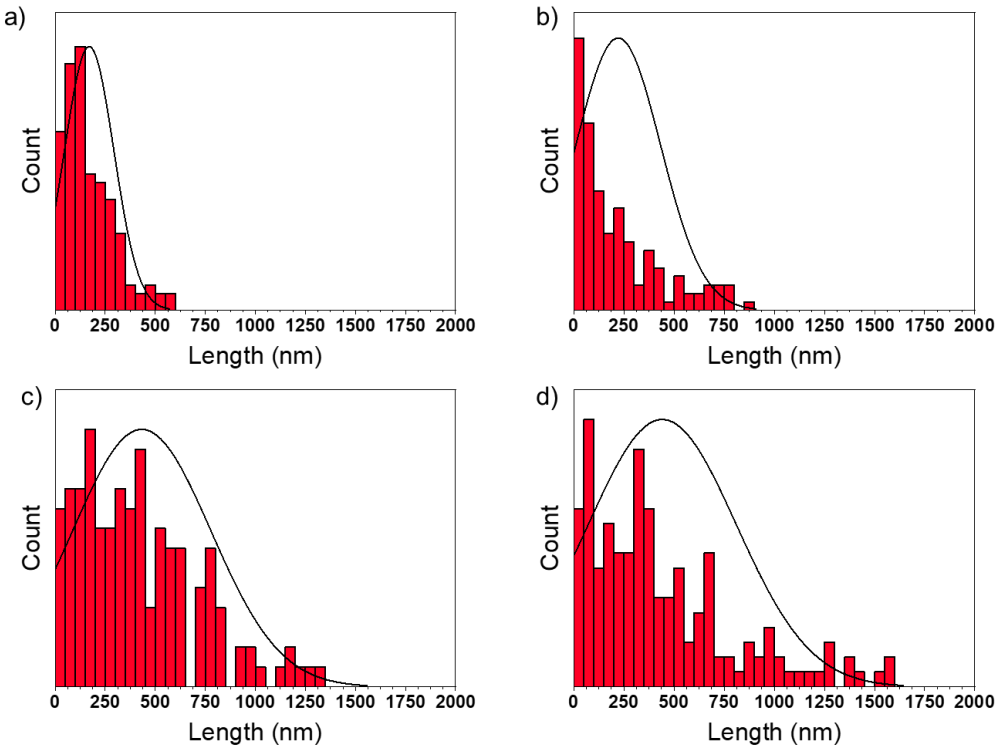


**Figure S27.** Histograms showing the nanofiber length distribution of P3HT$_{35}$-*b*-PPP$_{15}$ nanofibers in *n*BuAc (0.05 mg/mL) formed by self-nucleation suppressed seeded growth (50 °C) following solvent evaporation. Unimer-to-seed ratio $m_{unimer}/m_{seed}$ = **(a)** 1, **(b)** 2, **(c)** 3, and **(d)** 4. Final concentrations were 0.05 mg/mL.

**Table S2. Summary of data from self-nucleation suppressed seeded growth experiments of homogeneous P3HT$_{35}$-*b*-PPP$_{15}$ nanofibers (*n*BuAc, 0.1 mg/mL) at 50 °C. σ is standard deviation in $L_n$ measurements.**

| $m_{unimer}/m_{seed}$ | $L_n$ | $L_w$ | $Đ_L$ | σ |
|---|---|---|---|---|
| Seeds | 49 | 59 | 1.20 | 22 |
| 1 | 170 | 259 | 1.52 | 123 |
| 2 | 219 | 421 | 1.92 | 210 |
| 3 | 433 | 708 | 1.63 | 345 |
| 4 | 443 | 749 | 1.69 | 369 |

# References


(1) Pangborn, A. B.; Giardello, M. A.; Grubbs, R. H.; Rosen, R. K.; Timmers, F. J. Safe and Convenient Procedure for Solvent Purification. *Organometallics* **1996**, *15* (5), 1518–1520. https://doi.org/10.1021/om9503712.

(2) Standley, E. A.; Smith, S. J.; Müller, P.; Jamison, T. F. A Broadly Applicable Strategy for Entry into Homogeneous Nickel(0) Catalysts from Air-Stable Nickel(II) Complexes. *Organometallics* **2014**, *33* (8), 2012–2018. https://doi.org/10.1021/om500156q.

(3) Schneider, C. A.; Rasband, W. S.; Eliceiri, K. W. NIH Image to ImageJ: 25 Years of Image Analysis. *Nat. Methods* **2012**, *9* (7), 671–675. https://doi.org/10.1038/nmeth.2089.

(4) Usta, H.; Alimli, D.; Ozdemir, R.; Tekin, E.; Alkan, F.; Kacar, R.; Altas, A. G.; Dabak, S.;

Gürek, A. G.; Mutlugun, E.; Yazici, A. F.; Can, A. A Hybridized Local and Charge Transfer Excited State for Solution-Processed Non-Doped Green Electroluminescence Based on Oligo(p-Phenyleneethynylene). *J. Mater. Chem. C* **2020**, *8* (24), 8047–8060. https://doi.org/10.1039/d0tc01266a.

(5) Wu, S.; Bu, L.; Huang, L.; Yu, X.; Han, Y.; Geng, Y.; Wang, F. Synthesis and Characterization of Phenylene-Thiophene All-Conjugated Diblock Copolymers. *Polymer.* **2009**, *50* (26), 6245–6251. https://doi.org/10.1016/j.polymer.2009.11.001.

(6) Fukui, T.; Garcia-Hernandez, J. D.; MacFarlane, L. R.; Lei, S.; Whittell, G. R.; Manners, I. Seeded Self-Assembly of Charge-Terminated Poly(3-Hexylthiophene) Amphiphiles Based on the Energy Landscape. *J. Am. Chem. Soc.* **2020**, *142* (35), 15038–15048. https://doi.org/10.1021/jacs.0c06185.

(7) MacFarlane, L. R.; Li, X.; Faul, C. F. J.; Manners, I. Efficient and Controlled Seeded Growth of Poly(3-Hexylthiophene) Block Copolymer Nanofibers through Suppression of Homogeneous Nucleation. *Macromolecules* **2021**, *54* (24), 11269–11280. https://doi.org/10.1021/acs.macromol.1c02005.